

Landslides (2014) 11:897–907
 DOI 10.1007/s10346-013-0437-x
 Received: 7 August 2012
 Accepted: 8 October 2013
 Published online: 31 October 2013
 © Springer-Verlag Berlin Heidelberg 2013

Long Nguyen Thanh · Florimond De Smedt

Slope stability analysis using a physically based model: a case study from A Luoi district in Thua Thien-Hue Province, Vietnam

Abstract A case study of slope stability mapping is presented for the A Luoi district situated in the mountainous western part of Thua Thien-Hue Province in Central Vietnam, where slope failures occur frequently and seriously affect local living conditions. The methodology is based on the infinite slope stability model, which calculates a safety factor as the ratio between shear strength and shear stress. The triggering mechanism for slope instability considered in the analysis is the maximum daily precipitation recorded in a 28-year period (1976–2003) taking into account runoff and infiltration predicted with a hydrological model. All necessary physical parameters are derived from topography, soil texture, and land use, in GIS-raster grid format with pixel size of 30 by 30m. Results of the analysis are compared with a slope failure inventory map of 2001, showing that more than 86.9 % of the existing slope failures are well predicted by the physically based slope stability model. It can be concluded that the larger part of the study area is prone to landsliding. The resulting slope stability map is useful for further research and land-use planning, but for precise prediction of future slope failures, more effort is needed with respect to spatial variation of causative factors and analysis techniques.

Keywords Slope stability · Safety factor · Wetness index · Vietnam · Thua Thien-Hue · A Luoi

Introduction

Downslope movement of soil and rock under the direct influence of gravity, depends on several factors as geology, geomorphology, human impact, rainfall, etc. (e.g., Varnes 1978; Crozier 1986; Cruden and Varnes 1996). The identification of causative factors is the basis of many methods of slope stability assessment. These factors may be dynamic (e.g., pore-water pressure), or passive (e.g., rock structure) and may also be considered in terms of the roles they perform in destabilizing a slope (Crozier 1986). In this sense, the factors can be pre-conditioning factors (e.g., slope steepness), preparatory factors (e.g., deforestation), or triggering factors (e.g., rainfall). Overviews of environmental factors and their reliance for slope stability have been presented by Sidle and Ochiai (2006) and van Westen et al. (2008).

In most studies of landslides, the slope gradient is taken into account as the principal causative or triggering factor (e.g., Lohnes and Handy 1968; Swanston and Dyrness 1973; Ballard and Willington 1975). Slope gradients are sometimes considered as an index of slope stability, and can be numerically evaluated and depicted spatially when a digital elevation model (DEM) is available (e.g., O'Neill and Mark 1987; Gao 1993). Not only slope gradient is important for landsliding, but also other environmental factors exert major influences. For example, slope failure can occur even in particular regions of low-slope gradient, which

shows that geomorphic, hydrologic, geologic, pedologic, and possibly other factors are important determinants of slope stability as well.

Hydrology plays an important role in landslide initiation. Spatial patterns of rainfall are closely associated with landslide initiation (Campbell 1966; So 1971; Starkel 1976) by means of their influence to increase pore-water pressure in unstable hill slopes (Sidle and Swanston 1982; Sidle 1984; Iverson and Major 1987; Tsukamoto and Ohta 1988; Cascini et al. 2013). Some researchers concluded that rainfall intensity is the most important determinant (e.g., Sidle and Swanston 1982; Keefer et al. 1987; Aleotti 2004; Guzzetti et al. 2008); others found a correlation of long-term precipitation with landslide occurrences (e.g., Endo 1969; Glade 1998; Terlien 1998; Hong et al. 2005; Cardinali et al. 2006). Individual single rainstorms are likely to trigger shallow landslides, while deeper landslides need more antecedent precipitation (van Asch et al. 2009).

The most straightforward approach is the compilation of a landslide inventory, which, however, usually requires a lot of time and effort. Landslide inventory maps, derived from historic archives, field data collection, interviews, and image interpretation, are essential, but unfortunately, often lacking (van Westen et al. 2006). Guzzetti et al. (1994), Glade (2001), Petrucci and Polemio (2003) and Guzzetti (2000) discuss the use of historical data in natural hazard assessment. Generally, widely used methods for making a landslide inventory map are field investigations and remote sensing techniques. A wide range of both relative and absolute methods has been employed for dating of field evidence (Lang et al. 1999; Bull 1996). A number of papers dealing with the determination of frequency and magnitude of occurrence from field evidence can be found in Mathew et al. (1997).

Methods for modeling slope instability have been employed by different investigators throughout the world. Reviews outlining the methods are given by Brabb (1984), Varnes and the International Association of Engineering Geology Commission on Landslides and Other Mass Movements (1984), Hansen (1984), van Westen (1994), Carrara et al. (1995), Hutchinson (1995), Soeters and van Westen (1996), van Westen et al. (1997), Aleotti and Chowdhury (1999), Guzzetti et al. (1999), Gorsevski et al. (2003) and Fell et al. (2008). Physically based models for the assessment of landslide susceptibility rely upon the understanding of the physical laws controlling slope instability. A very popular approach is the one-dimensional infinite slope stability analysis (e.g., Montgomery and Dietrich 1994; Dietrich et al. 1995; Wu and Sidle 1995; Terlien et al. 1995; Pack et al. 1998; Dymond et al. 1999; Iverson 2000; Crosta and Dal Negro 2003; Godt et al. 2008; Capparelli and Versace 2011). In this approach, the stability of a slope is evaluated using parameters such as normal and tangent stresses, angle of internal friction, cohesion, pore-water pressure, soil weight, etc. Most commonly,

computation results in a factor of safety expressing the ratio between the local stabilizing and driving forces. Values greater than 1 indicate stability of the slope and values less than 1 identify unstable conditions. Despite the high potential, Sorbino et al. (2010) have shown that such models show some limitations related to the adopted simplifying assumptions, the quantity and quality of required data, and the quantitative interpretation of the results. Moreover, landslide-source areas obtained by physically based models may represent only part of mobilized soil volumes, such as in the case of debris avalanches (Cascini et al. 2012).

In this study, a case study is presented of infinite slope stability analysis to assess the spatial distribution of slope stability in A Luoi district, Thua Thien-Hue province, Central Vietnam, and model results are compared with an inventory of shallow landslides that occurred in the study area. This work is a continuation of the Ph.D. research of the principal author (Long 2008).

Theory

Slope stability can be expressed by a safety factor, which is the ratio between the parameters that prevent a slope from failing, i.e., shear strength, and those that make a slope fail, i.e., shear stress. There are a variety of methods for slope stability analysis that are based on the infinite slope model concept. In this study, the safety factor is evaluated as (e.g., Montgomery and Dietrich 1994; van Westen and Terlien 1996; Acharya et al. 2006; Ray and De Smedt 2009)

$$F = \frac{C_s + C_r}{\gamma_e D \sin \theta} + \left(\frac{1-m}{\gamma_e} \right) \frac{\tan \phi}{\tan \theta} \quad (1)$$

where F is the safety factor, C_s and C_r are the soil and root cohesion (kilonewton per square meter) depending on the soil and vegetation type respectively, γ_w is the unit weight of water (kilonewton per cubic meter), D is the thickness (meter) of the soil layer on top of the bedrock measured perpendicularly to the topographical surface, ϕ is the angle of internal friction (degree) of the soil, θ is the slope angle (degree), which in the infinite slope method, is assumed to coincide with the bedrock and water table slope angle, and γ_e is the effective unit weight (kilonewton per cubic meter) of soil and overburden given by

$$\gamma_e = \frac{q \cos \theta}{D} + m \gamma_s + (1-m) \gamma_d, \quad (2)$$

where γ_d is the dry unit weight (kilonewton per cubic meter) of the soil, γ_s is the saturated unit weight (kilonewton per cubic meter) of the soil, and q is any surcharge (kilonewton per square meter) on the soil surface. Parameter (m) in both equations is the wetness index, defined as the relative position of the water table h/D in the soil layer, where h is the thickness (meter) of the saturated part of the soil above the bedrock. The wetness index depends on hydrological conditions and soil and terrain characteristics. The geometry of the slope and the different variables in the above equations are illustrated in Fig. 1. All parameters in the above equations are spatially variable.

The triggering mechanism for slope instability is usually a rise of ground water increasing the saturation of the soil and pore-

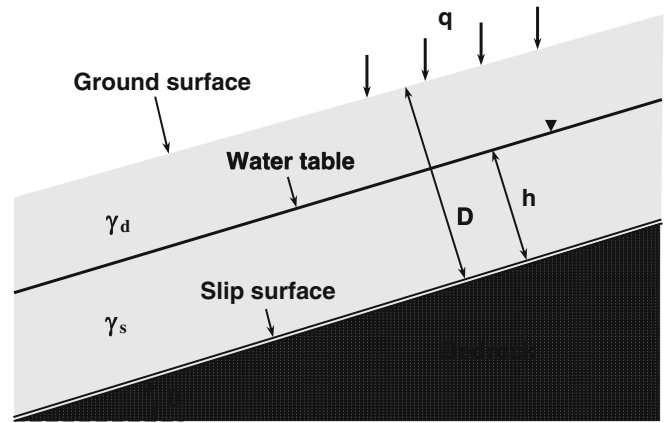


Fig. 1 Schematic representation of the infinite slope method, depicting relevant parameters and variables

water pressure. Simple models have been developed for estimating soil saturation as for instance presented by Montgomery and Dietrich (1994), Borga et al. (1998) and Pack et al. (1998). These approaches apply to shallow soils resting on bedrock, so that shallow lateral subsurface flow follows topographic gradients in equilibrium with rainfall infiltration and the contributing area to flow at any point is given by the specific catchment area defined from the surface topography, or

$$Khbsin\theta = IA, \quad (3)$$

where K is the hydraulic conductivity (meter per second) of the soil, b is the width of the considered groundwater flow section (meter), $\sin\theta$ stands for the hydraulic gradient, I is the infiltration rate (meter per second), and A is the specific catchment area (square meter). Although steady state is assumed, the rainfall rate used is not a long-term average of recharge, but rather an infiltration rate for a critical period of wet weather likely to trigger landslides (Pack et al. 1998). The infiltration rate can be determined as

$$I = (1-C)P, \quad (4)$$

where P is the precipitation rate (meter per second) and C is a runoff coefficient depending on land use, vegetation, soil texture, and slope angle. The spatial variation of the runoff coefficient is determined with the WetSpa hydrological model (Liu and De Smedt 2004), which has shown to predict runoff fairly well (e.g., Smith et al. 2012; Safari et al. 2012). Equations 3 and 4 enable to calculate the wetness index as

$$m = \frac{h}{D} = \frac{(1-C)PA_b}{KD\sin\theta}, \quad (5)$$

where $A_b = A/b$ is the specific catchment area per width (meter). Based on this equation, maps of the wetness index resulting from a particular rainfall event can be generated. The major advantage of the methodology is that it is parsimonious with respect to required data input and numerical computation time. Values of m should vary from 0 to 1; hence, if values of m determined with Eq. 5 exceed 1, they are set equal to 1. Hence, Eqs. 1 and 5 can be used to determine safety factor

Table 1 Landslide susceptibility classification based on the factor of safety (modified from Pack et al. 1998)

Safety factor	Slope stability class
$F > 1.5$	Stable slope
$1.5 > F > 1.25$	Moderately stable slope
$1.25 > F > 1$	Quasi-stable slope
$0.5 < F < 1$	Unstable slope
$0 < F < 0.5$	Very unstable slope

values, which can be reclassified into slope stability classes based on geomechanical principles, as shown in Table 1 modified from Pack et al. (1998). Pack et al. (1998) defined six stability classes, of which we kept the first three, i.e., stable slope ($F > 1.5$), moderately stable slope ($1.25 < F < 1.5$) and quasi-stable slope ($1 < F < 0.25$), and renamed the next two classes as unstable slope ($0.5 < F < 1$) and very unstable slope ($0 < F < 0.5$), while the last class ($F < 0$) was ignored as this is physically impossible.

Study area

The study area belongs to the A Luoi district in the mountainous western part of Thua Thien-Hue Province in Central Vietnam (Fig. 2). Slope failures occur frequently in this area and have a strong impact on local living conditions. For example, several

slope failures at the end of 1999 caused severe damage, more than 20 people lost their lives and many houses, roads, and other infrastructures were destroyed. Hence, spatial analysis of slope stability in this mountainous region is very important. The study area covers about 2,627 km² and altitude ranges from about 80 to 1,700 m. The west part is mountainous with strongly dissected and steep mountains ranging from 500 to 1,700 m in altitude, while the east part is more flat with plains and dispersed hills.

The tropical monsoon climate is generally hot and humid with an average annual precipitation of about 3,500 mm. On average, there are about 200 rainy days per year. The wet season lasts from September to December with many typhoons particularly in October and November. Daily precipitation has been recorded at two stations in A Luoi district for a 28-year period from 1976 to 2003. The maximum recorded rainfall was 610 and 759 mm per day, respectively, both observed on 5 November 1999, on the fifth day of a huge storm that lasted from 1 to 6 November 1999.

A shallow landslide occurrence map was extracted from an inventory of landslides in Thua Thien-Hue Province by Văn et al. (2001), which took 4 years (1998–2001) to be completed. Three main methods for landslide inventory mapping were employed as follows: (1) field recognizance to investigate landslide occurrences, (2) collection of historic information on landslides, and (3) interpretation of landslide occurrences from aerial photographs coupled with field verification. A total of 181 shallow landslides were identified as shown in Fig. 2. The average area of a landslide

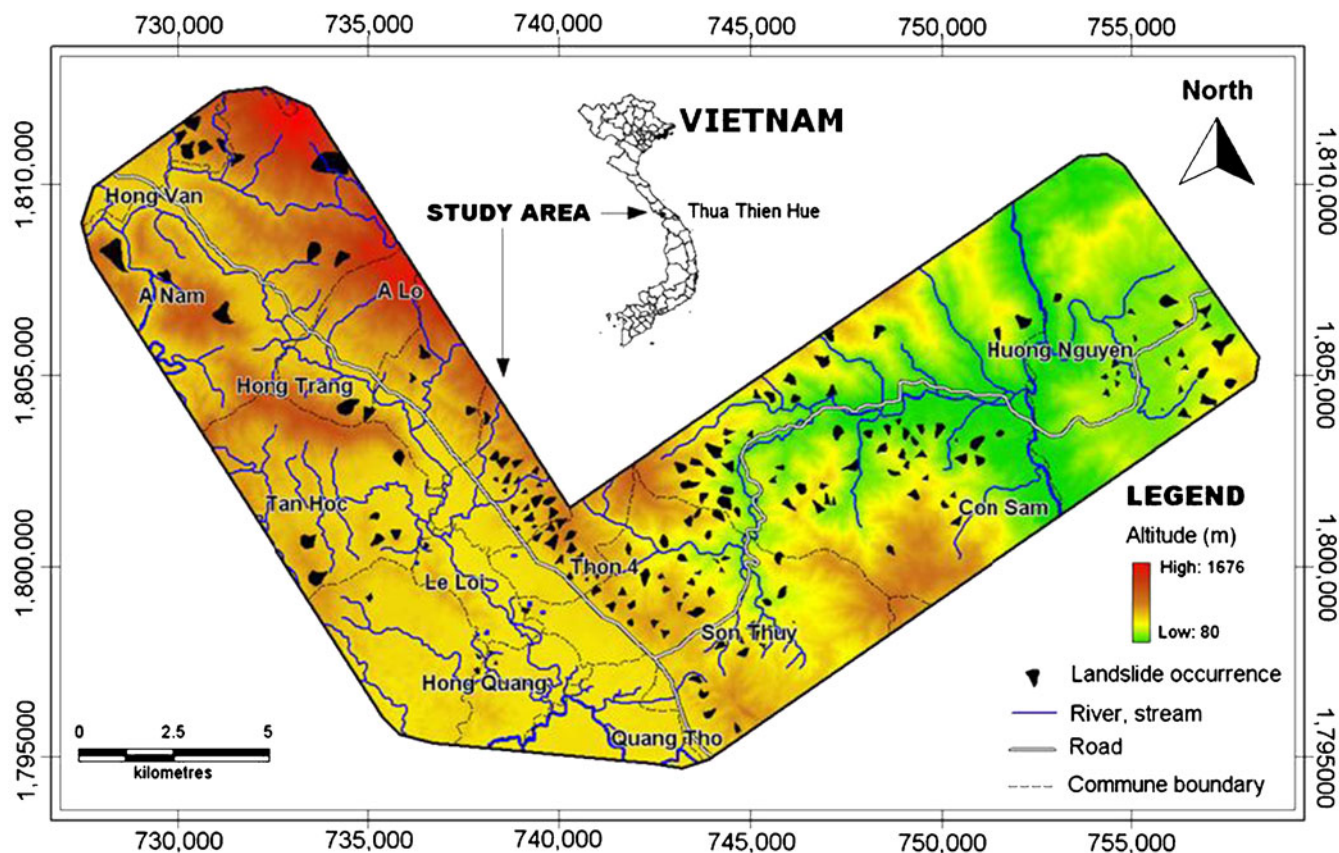


Fig. 2 Location and main characteristics of the study area in A Luoi district, Thua Thien-Hue Province, Central Vietnam; shown in the figure are UTM Zone 48 North coordinates (m), elevations (m), rivers and streams, main roads, and the shallow landslide inventory by Văn et al. (2001)

in the study area is approximately 4 ha and the depth ranges from 0.5 to 2 m. Some examples of recent landslides are shown in Fig. 3. Unfortunately, there is no information available on the date of occurrence and possible triggering of the slides by storm events. Also, no distinction was made between the location of onset of the landslides and the downslope accumulation of debris. Hence, the landslide inventory yields basic information needed for this study, although the information is rather incomplete and should be used with caution and reservation. However, from the location of the landslides, it is possible to identify some probable causes. Especially noticeable at the location of many slides are highly weathered soils, lack of vegetation, and steep slopes, often along roads. The typical landslides are shown in Fig. 3. Such slides happen each year during the rainy season.

Methodology

In order to calculate safety factors according to Eq. 1, all necessary parameters are derived from topography, soil texture, and land use. This information was compiled in the form of raster grid maps with a pixel size of 30 by 30 m. In order to build a DEM of the study area, the topographic map of Thua Thien-Hue Province on scale 1:50,000 (Cartographic Publishing House, Vietnamese Ministry of Natural Resources and Environment) was digitized. On the basis of elevation contours with intervals of 20 m, the DEM was derived by inverse distance interpolation using ILWIS 3.0 software. An impression of this DEM is shown in Fig. 2. A slope angle map was derived from the DEM using the slope function of ILWIS 3.0.

The soil map of Thua Thien-Hue Province on scale 1:50,000, dating from 2000 (Cartographic Publishing House, Vietnamese Ministry of Natural Resources and Environment), was digitized as shown in Fig. 4. This soil map was mapped in 1999 according to the Vietnamese soil classification scheme modified from FAO-UNESCO. Soils types are denoted by a two-letter code with indices as shown in the legend of Fig. 4, referring to soil type, parent material, soil texture, and soil depth. Vän et al. (2001) determined typical mechanical properties for each parent material and soil texture by laboratory analyses, such as dry and saturated soil unit weight, porosity, liquid limit, plasticity limit, plastic index, angle of internal friction, soil cohesion, compressibility, and hydraulic conductivity. The values of the parameters needed in this study, extracted from Vän et al. (2001), are listed in Table 2. Notice that in the study area, there are only three soil types: clay, clay loam, and loam, which originate from four different types of parent material: archaic alluvium, intrusive magma, metamorphic rock, and continental sediments. The soil depth on the soil map given in the form of classes, i.e., <math><0.3</math>, $0.3-0.5$, $0.5-0.7$, $0.7-1$, and >1 m, was converted to average values of each soil depth range. For the soil depth class >1 m, a value of 2 m was assigned, because this is a typical magnitude of soil thickness in the mountainous areas in Vietnam, for soils which have been suffering from strong weathering conditions (Fridland 1973). Moreover, none of the shallow landslides identified in the study area by Vän et al. (2001) were deeper than 2 m. On the basis of these assumptions, a grid map of approximate soil depth in the study area was created.

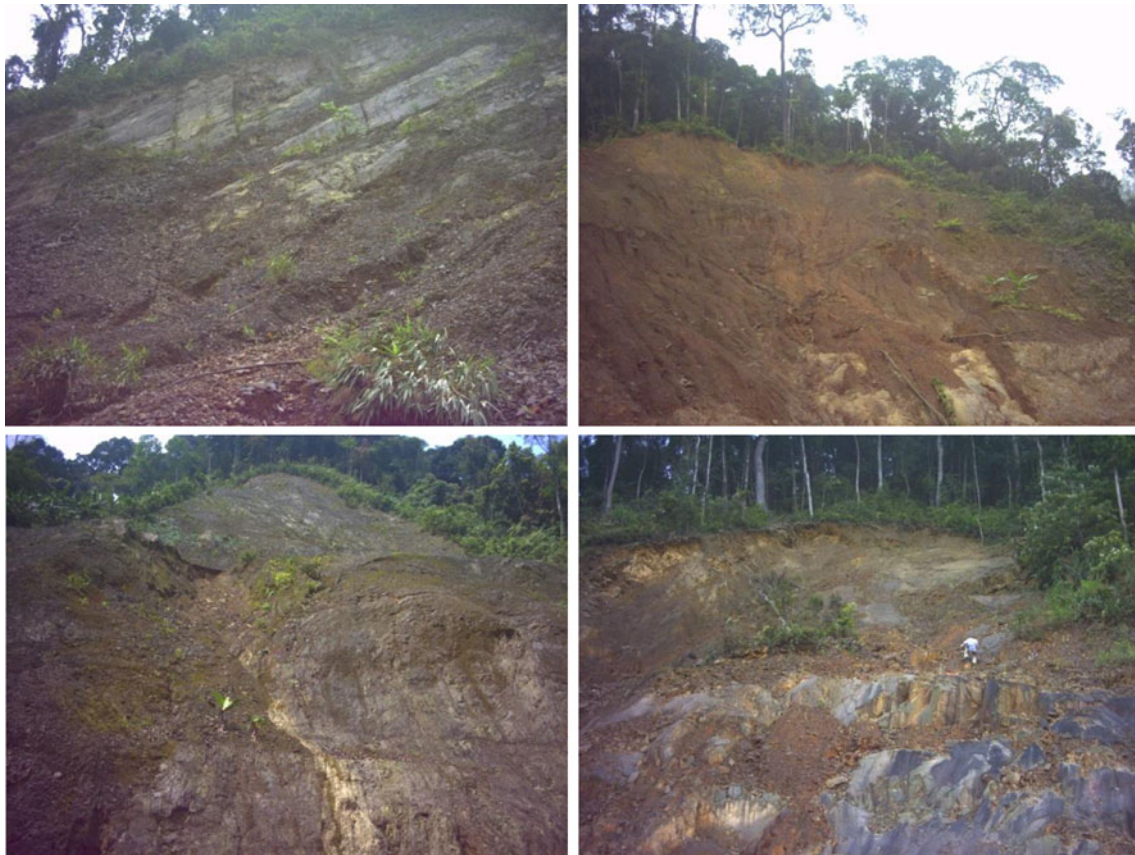
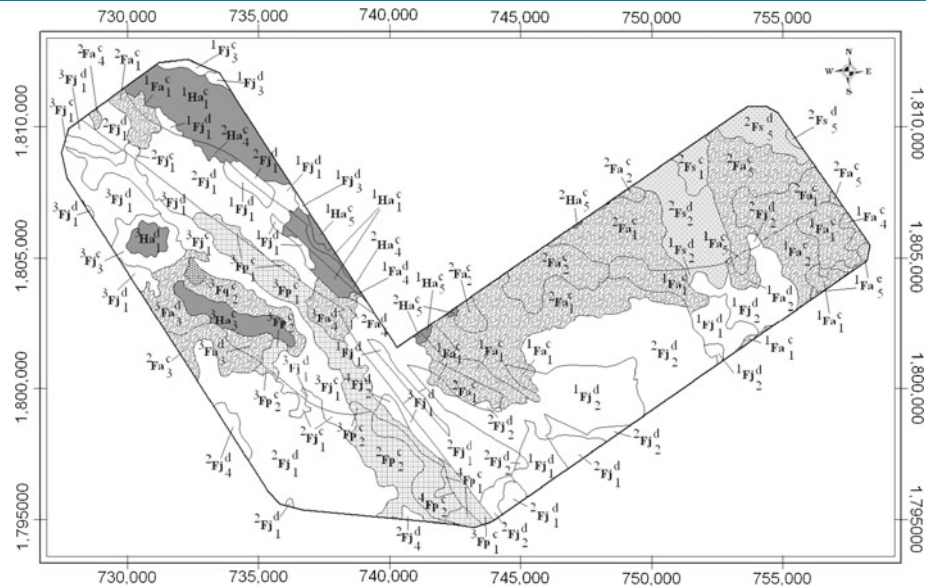


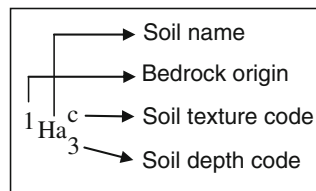
Fig. 3 Pictures of shallow landslide occurrences in the study area

Fig. 4 Soil map of the study area



LEGEND

Symbol explanation



Bedrock origin

1. Intrusive magma
2. Metamorphic rocks
3. Continental sediments
4. Archaic alluvium

Soil texture

- c. Loam
- d. Clay loam
- e. Clay

- Ha** Red humus soil mainly on magma rocks and sometimes on sediments
- Fa** Red yellow soils mainly on magma acid and metamorphic rocks
- Fj** Red yellow soils mainly on metamorphic claystones
- Fp** Brown yellow soil on continental sediments and ancient alluvium
- Fq** Light yellow soils mainly on sandstones
- Fs** Brown yellow soil mainly on claystones

Soil depth

1. > 1 m
2. 0.7–1 m
3. 0.5–0.7 m
4. 0.3–0.5 m
5. < 0.3 m

A land-use map of the study area was derived from a Landsat TM 5 image of February 20, 1999 (path/row: 125/48). Different types of land cover were identified using the Normalized Difference Vegetation Index and compared to field observations and photographs of Vän et al. (2001). The field descriptions were used as training sites in a supervised classification for quantitative assessment of the land cover. Four major land-use patterns were identified as follows: (1) villages and built-up area, (2) shrubs covered or bare soils, (3) afforested land, and (4) agricultural areas. The different land uses are shown in Fig. 5. The major land covers are afforested land (47.6 %) and shrub-covered or bare soils (48.7 %). The afforested areas are mainly acacia trees (*Acacia mangium* or *Acacia eucoliformic*), which have been planted since 1982. The harvest cycle for these acacia trees is commonly from 8 to 12 years, when the height is about 15 to 18 m and the root depth about 1 to 1.5 m (Hinh 1996; Hà 2008). Vegetation improves slope

stability in several ways, as for instance by interception of rainfall promoting evaporation and reducing water available for infiltration (Satterlund 1972; Greenway 1987) and by removing soil moisture through evapotranspiration leading to lower soil moisture levels (Dingman 1994), but primarily by providing root cohesion to the soil mantle (Wu et al. 1979; Gray and Megahan 1981; O’Loughlin and Ziemer 1982; Riestenberg and Sovonick-Dunford 1983; Greenway 1987). Root-induced cohesion is significant in slope stability only if the root density is high in the top 60 cm of the soil and is supported by strong tap roots (Styczen and Morgan 1995) and if the roots penetrate through the shear zone (Ocakoglu et al. 2002), which is certainly the case for the acacia trees and shallow landslides. Because exact values of the root cohesion of such trees in the study area are lacking, the root cohesion was adapted and modified from literature as 8 kNm^{-3} (Sidle 1991; Kayastha 2006; Vinh 2007), assumed to be valid over

Table 2 Soil parameters (Van et al. 2001)

Soil type		γ_d	γ_s	C_s	ϕ	K
Parent material	Texture	(kNm^{-3})	(kNm^{-3})	(kNm^{-2})	($^\circ$)	(ms^{-1})
Alluvium	Clay	15.1	18.9	4.2	21	1.9×10^{-7}
	Clay loam	15.8	18.5	3.0	25	6.4×10^{-7}
	Loam	16.9	19.3	1.8	22	1.5×10^{-6}
Intrusive magma	Clay	15.2	18.3	2.3	24	3.0×10^{-6}
	Clay loam	14.2	17.9	2.1	24.5	1.2×10^{-5}
	Loam	18.1	19.1	1.9	30	4.3×10^{-4}
Metamorphic	Clay	13.7	17.9	1.3	24	1.6×10^{-6}
	Clay loam	15.2	18.2	0.9	26	1.9×10^{-5}
	Loam	14.8	15.8	0.9	21	1.3×10^{-4}
Continental sediments	Clay	15.1	18.2	4.4	19	1.2×10^{-6}
	Clay loam	15.5	18.6	2.6	23	3.1×10^{-6}
	Loam	15.0	19.3	0.9	21	1.3×10^{-4}
	Clay	15.1	18.9	4.2	21	1.9×10^{-7}

γ_d dry unit weight, γ_s saturated unit weight, C_s soil cohesion, ϕ angle of internal friction, K hydraulic conductivity

the entire soil depth. A less important effect of trees is the surcharge induced by their weight. Surcharge increases the downslope forces on a slope, but also increases the frictional

resistance of the soil. For vegetation, this is significant only for trees, as the weight of most other plant species is too small (Styczen and Morgan 1995). Again, exact values for the study area

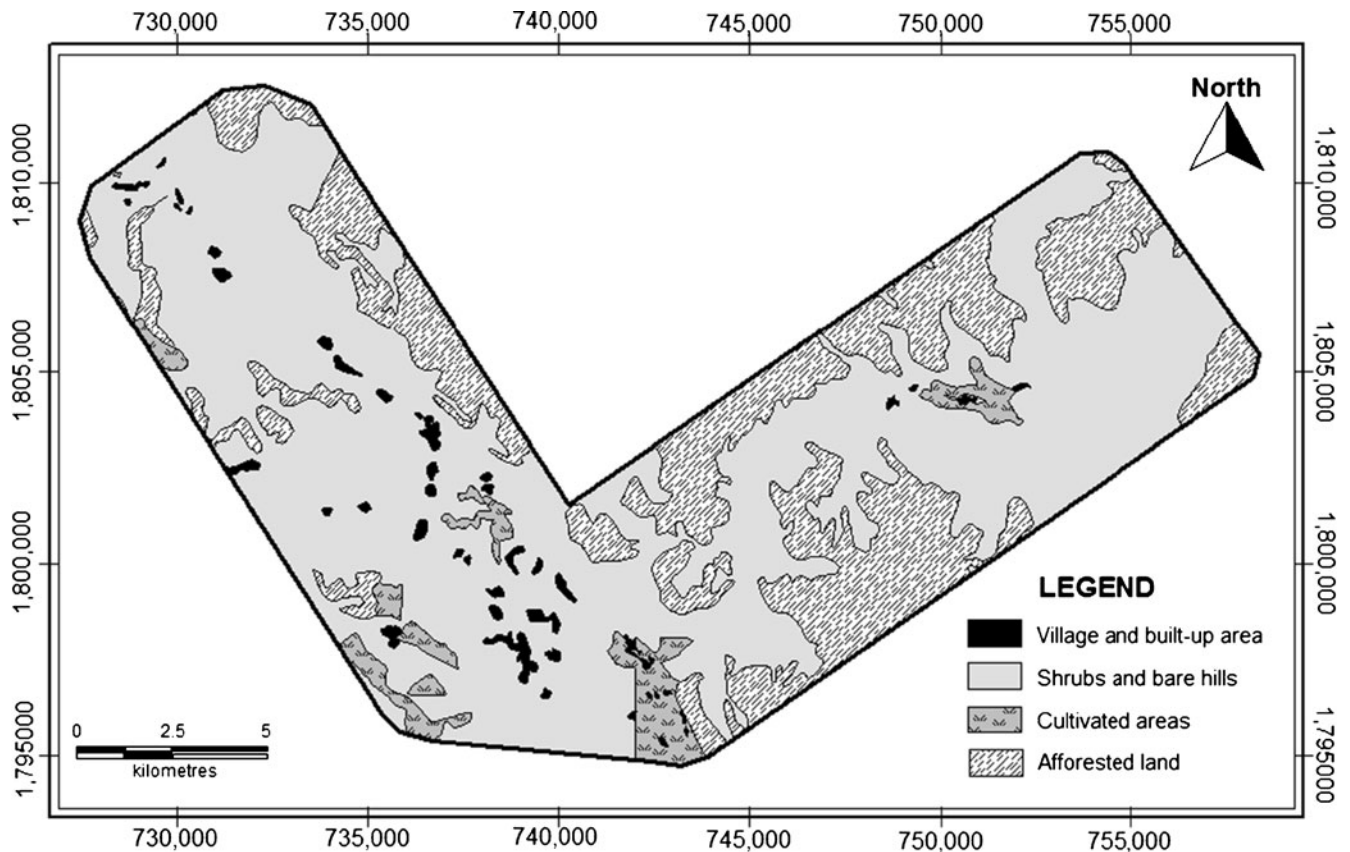


Fig. 5 Land-use map of the study area derived from a Landsat TM 5 image of 20 February 1999; major land covers are afforested land (47.6 %) and shrub-covered or bare soils (48.7 %)

are lacking, and one has to rely on what can be found in the literature. In view of the type of trees, their average height and age, a value of 0.7 kNm^{-2} was adopted for the surcharge (Kayastha 2006; Vinh 2007). Wind forces on trees were ignored, although these can be a major triggering factor of slope failure. Based on the land-use map and the attribute values, maps of root cohesion and surcharge were created by the “Map attribute” function of ILWIS.

In order to calculate the infiltration rate according to Eq. 5, raster grid maps of runoff coefficient and precipitation rate were derived, also with a pixel size of 30 by 30 m. For the precipitation rate, it was decided to use an extreme value as a worst-case scenario that likely could initiate landslides, i.e., the maximum daily rainfall recorded in the different stations in the district. A spatial distribution map of this rainfall was constructed using inverse distance weighing method. The runoff coefficient map was determined with the WetSpa model and the digital maps of topography, soil texture, and land use assuming that the soil surface was saturated, which is justified as the maximum rainfall occurred on the fifth day of a huge storm.

Results and discussion

Slope stability analysis for the study area is performed with the physical slope stability model given by Eq. 1. All parameters in the model are spatial variables including the wetness index, which can be evaluated with Eq. 5 depending upon hydrological and hydrogeological conditions. The runoff coefficients determined with the WetSpa model are shown in Fig. 6. The values range between 0.3 and 1, depending on land

use, soil type, and slope angle. Some of these features are clearly noticeable on the map, especially the spatial patterns of soil type (Fig. 4) and land use (Fig. 5). High runoff coefficients are found on clayey soils with steep slopes and land-use village and build-up area, or shrubs and bare hills, while small values are obtained for loamy soils, faint slopes, and afforested land.

Based on the maximum observed rainfall intensity in the study area and the runoff coefficients, infiltration rates are derived with Eq. 4 and subsequently, the wetness index with Eq. 5. A map of the resulting wetness index is given in Fig. 7, with values ranging between 0 and 1. A value of 1 implies completely saturated soils, which, during a heavy storm would typically occur in valleys, but are likely not to become unstable because of the smaller slope angles. On the other hand, small values for the wetness index are found on upper and steeper slopes, typically ridges, cliffs, or incisions by roads, which in case, covered by soil are more prone to become unstable. Hence, whether they obtained wetness index values can provoke slope instability still remains to be ascertained taking into account other properties related to actual shear stress and strength.

With the wetness index map, landslide safety factors are determined using Eq. 1. The obtained values range between 0.1 and 500. When classified according to the critical F values given in Table 1, a landslide susceptibility map is obtained as shown in Fig. 8. Results are also shown in Table 3, where the areas of the slope stability classes are given together with the observed shallow landslides areas contained in each class. The last column of Table 3

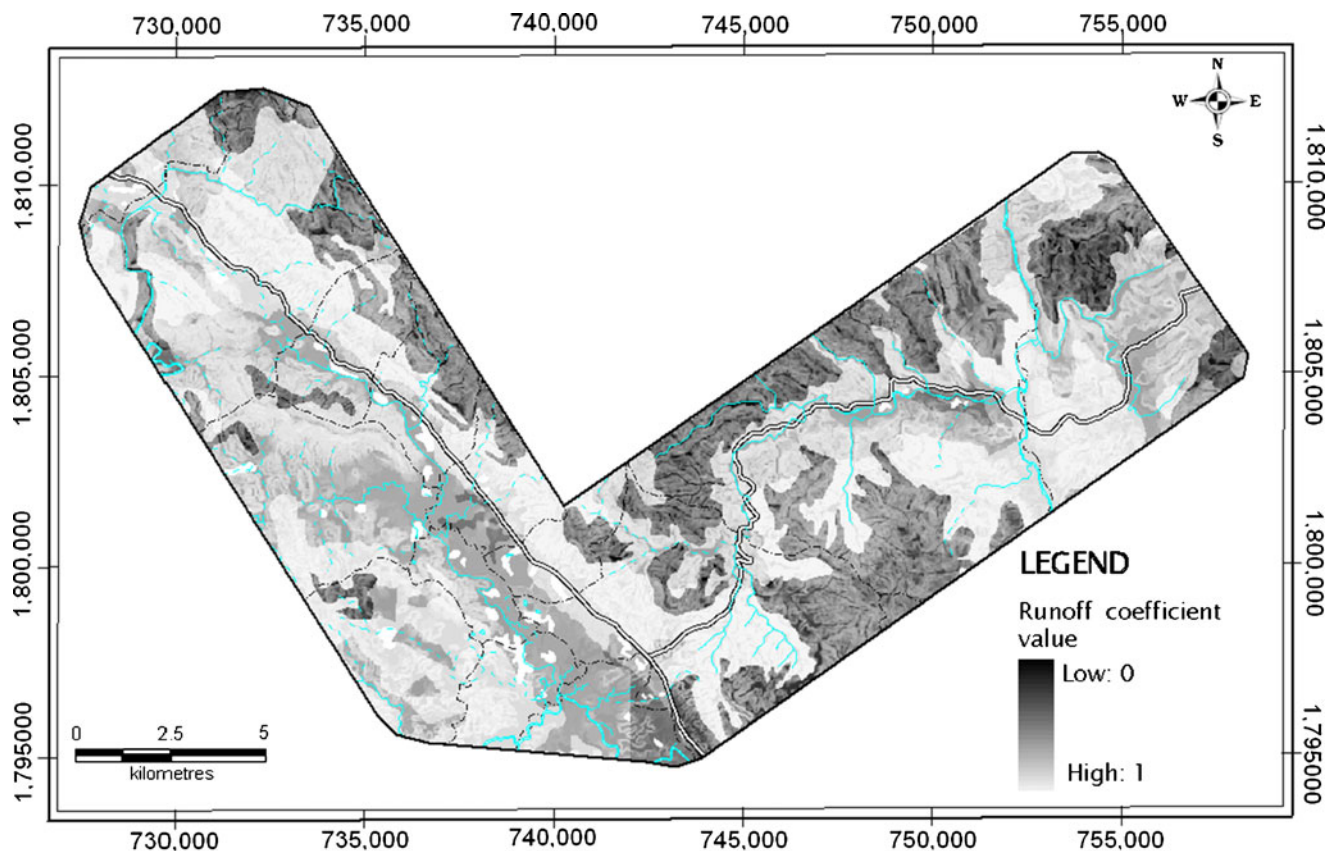


Fig. 6 Spatial distribution of the runoff coefficient derived with the WetSpa hydrological model

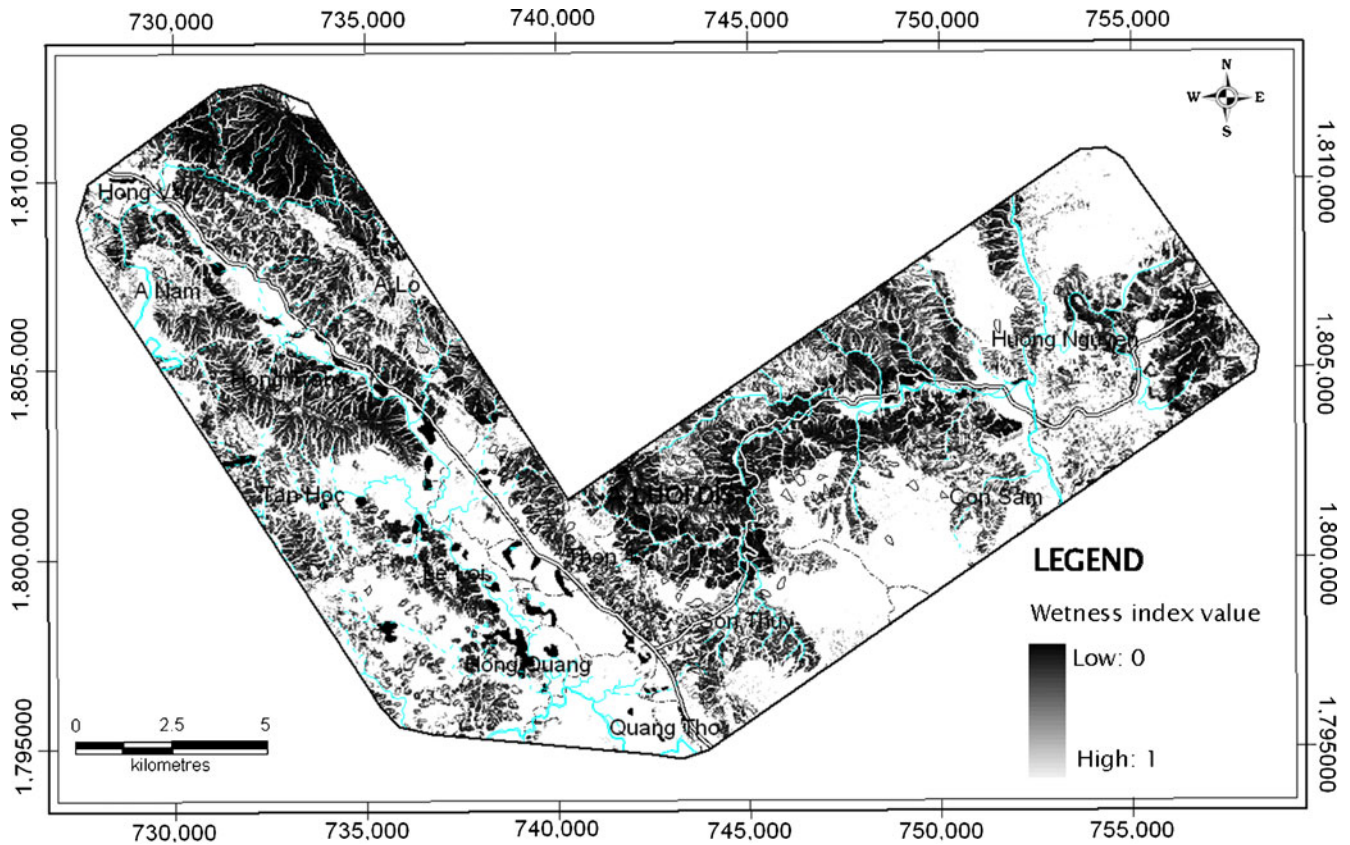


Fig. 7 Wetness index map resulting from a the maximum rainfall, observed on 5 November 1999, during a 28-year period (1976–2003)

gives the landslide density, i.e., ratio of observed shallow landslides area and corresponding area of the slope stability class. A large part of the area (47.9 %) is situated in the unstable and very unstable slope classes, which correspond to safety factors smaller than 1. These areas consist mostly of strongly dissected and steep mountains, which are often bare or covered by sparse vegetation like shrubs, although several parts are also afforested. The very unstable and unstable slope classes cover 67.0 % of the observed shallow landslides. The fair agreement between observed slope failures and predicted unstable and very unstable slope classes is also clearly seen in Fig. 8. The very unstable slope class ($F < 0.5$) is rather small, as it covers only 11.0 % of the study area and 15.9 % of the observed slope failures, and appears mostly on the very steep mountainsides. The largest class are the unstable slopes ($0.5 < F < 1$), which cover 36.9 % of the study area and 51.1 % of the observed slope failures. Notice that the landslide density is only slightly larger for the very unstable slope class compared to the unstable slope class.

On the other hand, the stable slope class covers 37.0 % of the study area and still 13.1 % of the observed slope failures. However, the landslide density is only 0.9 %, which is considerably less than the landslide density of the other classes and the 2.7 % average landslide density. The stable slope class is largely situated in the valleys along the main river courses, where also all villages are located and most cultivated areas. The main reason that slope failures are present in the stable slope class is that during the inventory, no distinction has been made between the location of onset of a landslides and the location of accumulation of the

debris. Hence, the usually flatter areas where debris accumulated have also been denoted as being part of a landslide.

The remaining areas are the quasi-stable and moderately stable slope classes. Both are rather small in extent, respectively, 9.5 and 5.6 % of the study area, but cover a somewhat larger percentage of the observed slope failures, i.e., 13.2 and 6.7 %. From physical point of view, these classes should have stable slopes as the factor of safety is larger than 1. However, in order to take into account data uncertainty but mainly to compensate for the simplifying assumptions inherent in the infinite slope stability approach, the factor of safety should be larger than 1, say 1.5 as proposed by Pack et al. (1998). Hence, the quasi-stable and moderately stable slope classes, with F values between 1 and 1.5, are also prone to slope failure, although to a lesser extent than the unstable and very unstable slope classes. This is reflected in the landslide density percentages that decrease from 3.9 % for the very unstable slope class to 3.2 % for the moderately stable slope class.

Overall, the slope classes with a safety factor less than 1.5 cover 86.9 % of the observed shallow landslides in the study area. The remaining observed landslides not predicted by the model are located in the stable stability class, very likely because the landslide inventory makes no distinction between failure area and deposition zone. Hence, the model results are fair in view of the uncertainty in the methodology and data. However, the predictive power is less, because there is little differentiation as all slope classes with a safety factor less than 1.5 cover 63.0 % of the study area. This is also evident from the obtained landslide densities, given in the last column of Table 3. The landslides

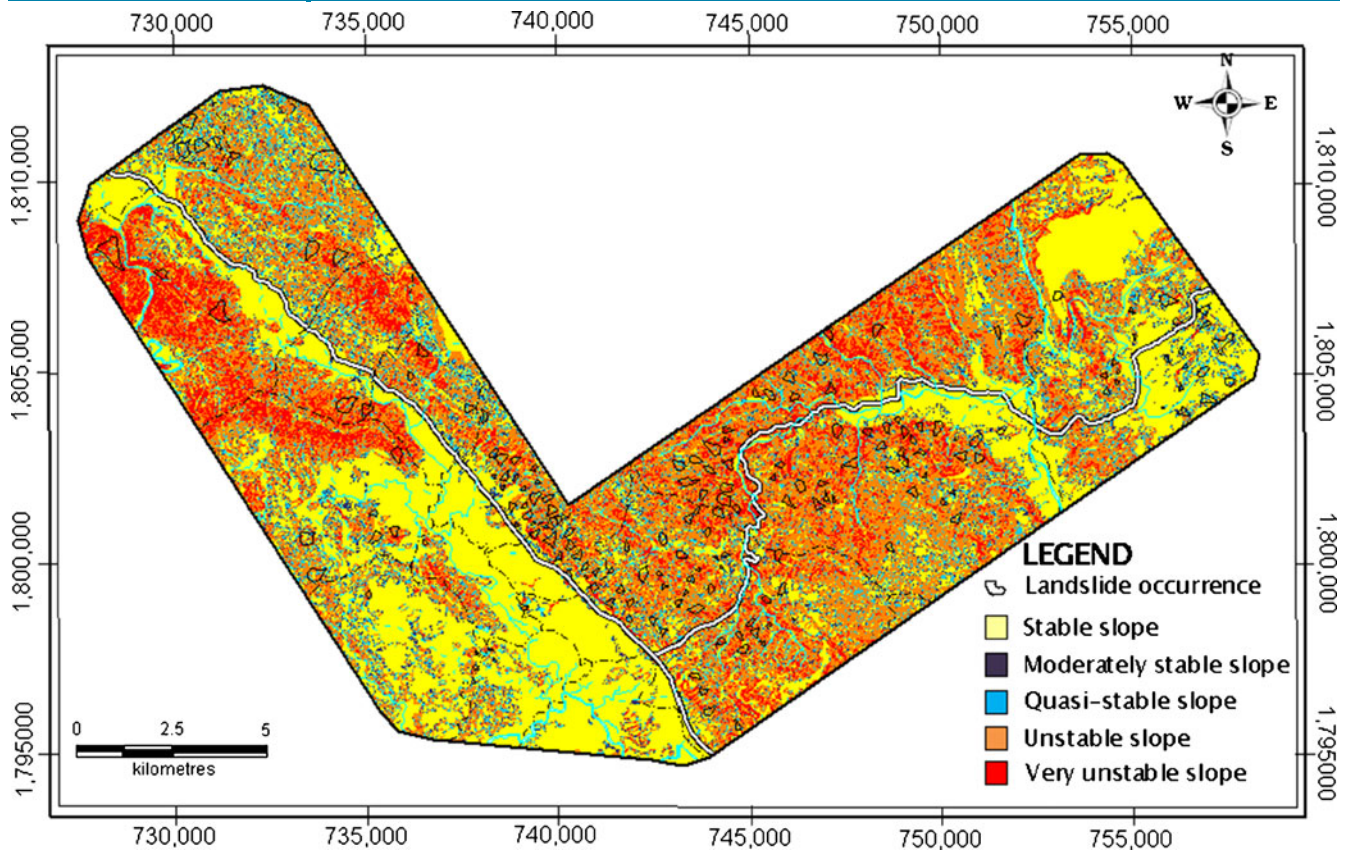


Fig. 8 Map of slope stability classes based on the factor of safety and stability classes as defined in Table 1

density values decrease from 3.9 % for the very unstable slope class to 0.9 % for the stable slope class, while the average landslide density for the whole study area combined is 2.7 %. Although the landslide density for the stable slope class is much less than the average value, which implies that the predictive power of the stable slope class is quite good, the landslide density for the other slope classes are only somewhat larger the average value, which considerably restricts their predictive power. Moreover, the results obtained (Table 3) show that the proposed methodology also lacks of predictive capability to differentiate between the unstable slope classes, as the observed landslide density varies from 3.9 % for the very unstable slope class to 3.2 % for the moderately stable slope class. Hence, these results are not really encouraging.

Conclusions

In this study, slope stability was investigated in A Luoi district in the mountainous western part of Thua Thien-Hue Province in Central Vietnam. The goal of the present work was to focus on the methodology, and explain the observed shallow landslides and derive useful information for future research and land-use planning. Slope stability was evaluated with the infinite slope stability model and results were compared with an inventory of shallow landslides. The triggering mechanism for slope instability considered in the analysis was the maximum daily precipitation recorded in a 28-year period (1976–2003) in the study area. In order to derive infiltration rates and the resulting wetness index, runoff coefficients were taken into account determined with the

Table 3 Area percentage of different slope stability classes and corresponding areal percentages of observed shallow landslides

Slope stability class	Area		Landslide area		Landslide Density (%)
	(km ²)	(%)	(km ²)	(%)	
Very unstable slope	28.9	11.0	1.1	15.9	3.9
Unstable slope	96.9	36.9	3.6	51.1	3.7
Quasi-stable slope	25.1	9.5	0.9	13.2	3.6
Moderately stable slope	14.7	5.6	0.5	6.7	3.2
Stable slope	97.1	37.0	0.9	13.1	0.9
Total	262.7	100	7.0	100	2.7

WetSpa hydrological model. All other necessary spatially distributed physical parameters were derived from digital maps of topography, soil texture, and land use. Results of the analysis compare favorably with the landslide inventory occurrence map, as 86.9 % of the observed slope failures are accurately predicted with a safety factor less than 1.5. It can be concluded that the larger part of the study area is prone to landsliding. These areas are generally mountainous and characterized by steep slopes, bare or covered by bush, or partly also afforested. The produced slope stability map can be considered as a first step in understanding the mechanisms and causes of slope failure in the study area, and as such, is useful for further research and land-use planning. However, for precise prediction of future slope failures, more effort is needed with respect to inventory, spatial variation of causative factors, and analysis techniques.

All data used in the analysis was gathered in the late 1990s and the spatial variation of geotechnical, hydrological, and vegetation parameters was greatly simplified. Also, for such a large area, it is very difficult to represent soil depth in a reliable manner. These deficiencies are reflected in the obtained results, as for instance can be noted in the runoff coefficient map and more importantly, because there is little differentiation in the predicted landslide density of the slope stability classes with safety factors less than 1.5. Hence, improving the quality of the data should be the first step in further research. Also, land-use changes that meanwhile occurred, as for instance, the growth and harvesting of the Acacia trees, need to be taken into account for prediction of future slope failures. Moreover, an updated inventory of slope failures would be most appropriate to validate/assess the reliability of the soil stability map derived in this research.

Acknowledgments

The authors would like to thank the anonymous reviewers for their useful comments and suggestions, which enabled to improve the quality of the paper.

References

- Acharya G, De Smedt F, Long NT (2006) Assessing landslide hazard in GIS: a case study from Rasuwa, Nepal. *Bull Eng Geol Environ* 65:99–107
- Aleotti P, Chowdhury R (1999) Landslide hazard assessment: summary, review and new perspectives. *Bull Eng Geol Environ* 58:21–44
- Aleotti P (2004) A warning system for rainfall-induced shallow failures. *Eng Geol* 73:247–265
- Ballard TM, Willington RP (1975) Slope instability in relation to timber harvesting in the Chilliwack Provincial Forest. *Forestry Chron* 51:59–62
- Borga M, Fontana GD, De Ros D, Marchi L (1998) Shallow landslide hazard assessment using a physically based model and digital elevation data. *Environ Geol* 35:81–88
- Brabb EE (1984) Innovative approaches to landslide hazard mapping. *Proceedings 4th International symposium on landslides, Toronto, 16–21 September 1984*, pp 307–324
- Bull WB (1996) Prehistorical earthquakes on the Alpine fault, New Zealand. *J Geophys Res* 101:6037–6050
- Campbell AP (1966) Measurement of movement of an earthflow. *Soil Water* 2:23–24
- Capparelli G, Versace P (2011) FlaIR and SUSHI: two mathematical models for early warning of landslides induced by rainfall. *Landslides* 8(1):67–79
- Cardinali M, Galli M, Guzzetti F, Ardizzone F, Reichenbach P, Bartoccini P (2006) Rainfall induced landslides in December 2004 in Southwestern Umbria, Central Italy. *Nat Hazard Earth Syst Sci* 6:237–260
- Cascini L, Cuomo S, Pastor M (2012) Geomechanical modelling of debris avalanches inception. *Landslides*. doi:10.1007/s10346-012-0366-0

- Cascini L, Sorbino G, Cuomo S, Ferlisi S (2013) Seasonal effect of rainfall on the shallow pyroclastic deposits of the Campania region (southern Italy). *Landslides*. doi:10.1007/s10346-013-0395-3
- Carrara A, Cardinali M, Guzzetti F, Reichenbach P (1995) GIS technology in mapping landslide hazard. In: Carrara A, Guzzetti F (eds) *Geographical information systems in assessing natural hazards*. Kluwer Academic Publishers, Dordrecht, pp 135–175
- Costa GB, Dal Negro P (2003) Observations and modelling of soil slip–debris flow initiation processes in pyroclastic deposits: the Sarno 1988 event. *Nat Hazards Earth Syst Sci* 3:53–69
- Crozier MJ (1986) *Landslides: causes, consequences and environment*. Croom Helm, London
- Cruden DM, Varnes DJ (1996) Landslide types and processes. In: Turner AK, Schuster RL (eds) *Landslides—investigation and mitigation*. National Research Council, USA, pp 36–75
- Dietrich WE, Reiss R, Hsu ML, Montgomery DR (1995) A process-based model for colluvial soil depth and shallow landsliding using digital elevation data. *Hydrol Process* 9:383–400
- Dingman SL (1994) *Physical hydrology*. Macmillan, New York
- Dymond JR, Jessen MR, Lovell LR (1999) Computer simulation of shallow landsliding in New Zealand hill country. *Int J App Earth Obs Geoinf* 1:122–131
- Endo T (1969) Probable distribution of the amount of rainfall causing landslides. *Annual Report 1968 Hokkaido Branch, For Exp Stn, Sapporo, Japan*, pp 122–136
- Fell R, Corominas J, Bonnard C, Cascini L, Leroy E, Savage WZ on behalf of the JTC-1 Joint Technical Committee on Landslides and Engineered Slopes (2008) Guidelines for landslide susceptibility, hazard and risk zoning for land use planning. *Eng Geol* 102:85–98
- Fridland VM (1973) *Soils and humid tropical weathering (in Vietnamese)*. Crust Scientific and Technological Publishing House, Hanoi
- Gao J (1993) Identification of topographic settings conducive to landsliding from DEM in Nelson County. *Earth Surf Process Landform* 18:579–591
- Glade T (1998) Establishing the frequency and magnitude of landslide–triggering rainstorm events in New Zealand. *Environ Geol* 35:160–174
- Glade T (2001) Landslide hazard assessment and historical landslide data—an inseparable couple? In: Glade T, Albini P, Francés F (eds) *The use of historical data in natural hazard assessments*. Kluwer, Dordrecht, pp 153–168
- Godt JW, Baum RL, Savage WZ, Salciarini D, Schulz WH, Harp EL (2008) Transient deterministic shallow landslide modeling: requirements for susceptibility and hazard assessments in a GIS framework. *Eng Geol* 102:214–226
- Gorsevski PV, Gessler PE, Jankowski P (2003) Integrating a fuzzy k–means classification and a Bayesian approach for spatial prediction of landslide hazard. *J Geogr Syst* 5:223–251
- Gray DH, Megahan WF (1981) Forest vegetation removal and slope stability in the Idaho Batholith. *USDA Forest Service Paper INT-127*
- Greenway DR (1987) Vegetation and slope stability. In: Anderson MG, Richards KS (eds) *Slope stability, geotechnical engineering and geomorphology*. John Wiley & Sons, Chichester, pp 187–230
- Guzzetti F (2000) Landslide fatalities and the evaluation of landslide risk in Italy. *Eng Geol* 58:89–107
- Guzzetti F, Cardinali M, Reichenbach P (1994) The AVI project: a bibliographical and archive inventory of landslides and floods in Italy. *Environ Manag* 18:623–633
- Guzzetti F, Carrara A, Cardinali M, Reichenbach P (1999) Landslide hazard evaluation: a review of current techniques and their application in a multi-scale study, central Italy. *Geomorphol* 31:181–216
- Guzzetti F, Peruccacci S, Rossi M, Stark CP (2008) The rainfall intensity–duration control of shallow landslides and debris flows: an update. *Landslides* 5(1):3–17
- Hà PT (2008) Asexual selection of *Acacia auriculiformis* with high productivity and quality for afforesting in some provinces in the Northern part of Vietnam. *Dissertation, Thai Nguyen University of Agriculture and Forestry*
- Hansen A (1984) Landslide hazard analysis. In: Brunnsden D, Prior DB (eds) *Slope instability*. John Wiley and Sons, New York, pp 523–602
- Hinh VT (1996) Growing progress table of acacia. *Forestry University, Vietnam*
- Hutchinson JN (1995) Keynote paper: landslide hazard assessment. In: Bell DH (ed) *Landslides*. Balkema, Rotterdam, pp 1805–1841
- Hong Y, Hiura H, Shino K, Sassa K, Suemine A, Fukuoka H, Wang G (2005) The influence of intense rainfall on the activity of large-scale crystalline schist landslides in Shikoku Island, Japan. *Landslides* 2(2):97–105
- Iverson RM (2000) Landslide triggering by rain infiltration. *Water Resour Res* 36:1897–1910

- Iverson RM, Major JJ (1987) Rainfall, ground–water flow, and seasonal movement at Minor Creek landslide, northwestern California: physical interpretation of empirical relation. *Geol Surv Am Bull* 99:579–594
- Kayastha P (2006) Slope stability analysis using GIS on a regional scale. Dissertation, Vrije Universiteit Brussel
- Keefer DK, Wilson RC, Mark RK, Brabb EE, Brown WM, Ellen SD, Harp EL, Wieczorek GF, Alger CS, Zatkun RS (1987) Real-time landslide warning during heavy rainfall. *Sci* 238:921–925
- Liu Y, De Smedt F (2004) WetSpa extension, documentation and user manual. Dept. Hydrology and Hydraulic Engineering. Vrije Universiteit Brussel, Belgium
- Lang A, Moya J, Corominas J, Schrott L, Dikau (1999) Classic and new dating methods for assessing the temporal occurrence of mass movements. *Geomorphol* 30:33–52
- Long NT (2008) Landslide susceptibility mapping of the mountainous area in A Luoi district, Thua Thien-Hue province. Vrije Universiteit Brussel, Vietnam
- Lohnes RA, Handy RL (1968) Slope angles in friable loess. *Geol J* 76:247–258
- Mathew JA, Brunson D, Frenzel B, Gläser B, Weiß MM (1997) Rapid mass movement as a source of climatic evidence for the Holocene. *Publisher Paläoklimaforschung – Palaeoclimate Research* 19, Stuttgart
- Montgomery DR, Dietrich WE (1994) A physically–based model for the topographic control on shallow landsliding. *Water Resour Res* 30:1153–1171
- Ocakoglu F, Gokceoglu C, Ercanoglu M (2002) Dynamics of a complex mass movement triggered by heavy rainfall: a case study from NW Turkey. *Geomorphol* 42:329–341
- O'Loughlin CL, Ziemer RR (1982) The importance of root strength and deterioration rates upon edaphic stability in steepland forests, in Carbon uptake and allocation in subalpine ecosystems as a key to management. *Proc IUFRO Workshop, Corvallis*, 2–3 August 1982, pp 70–78
- O'Neill MP, Mark DM (1987) On the frequency distribution of land slope. *Earth Surf Process Landform* 12:127–136
- Pack RT, Tarboton DG, Goodwin CN (1998) The SINMAP approach to terrain stability mapping. *Proceedings of 8th Congress of the International Association of Engineering Geology, Vancouver*, 21–25 September 1998, pp 1157–1165
- Petrucci O, Polemio M (2003) The use of historical data for the characterisation of multiple damaging hydrogeological events. *Nat Hazards Earth Syst Sci* 3:17–30
- Ray RL, De Smedt F (2009) Slope stability analysis on a regional scale using GIS: a case study from Dhading, Nepal. *Environ Geol* 57:1603–1611
- Riesterberg MM, Sovonick–Dunford S (1983) The role of woody vegetation in stabilizing slopes in the Cincinnati area, Ohio. *Bull Geol Soc Am* 94:506–518
- Safari A, De Smedt F, Moreda F (2012) WetSpa model application in the Distributed Model Intercomparison Project (DMIP2). *J Hydrol* 418–419:78–89
- Satterlund DR (1972) *Wildland watershed management*. Ronald Press, New York
- Sidle RC (1984) Shallow groundwater fluctuations in unstable hill slopes of coastal Alaska. *Z Gletscherkunde Glazialgeologie* 20:79–95
- Sidle RC (1991) A conceptual model of changes in root cohesion in response to vegetation management. *J Environ Qual* 20:43–52
- Sidle RC, Swanston DN (1982) Analysis of a small debris slide in coastal Alaska. *Can Geotec J* 19:167–174
- Sidle RC, Ochiai H (2006) *Landslides: processes, prediction, and land use*. American Geophysical Union, *Water Resources Monograph* 18, Washington
- Smith BM, Zhang Z, Zhang Y, Reed SM, Cui Z, Moreda F, Cosgrove BA, Mizukami N, Anderson EA, DMIP 2 Participants (2012) Results of the DMIP 2 Oklahoma experiments. *J Hydrol* 419–419:17–48
- So CL (1971) Mass movements associated with the rainstorm of June 1966 in Hong Kong. *Trans Inst Br Geogr* 53:55–65
- Soeters R, van Westen CJ (1996) Slope instability recognition, analysis, and zonation. In: Turner AK, Schuster RL (eds) *Landslides Investigation and Mitigation*. National Academy Press, Washington, pp 129–177
- Sorbino G, Sica C, Cascini L (2010) Susceptibility analysis of shallow landslides source areas using physically based models. *Nat Hazards* 53:313–332
- Starkel L (1976) The role of extreme (catastrophic) meteorological events in the contemporary evolution of slopes. In: Derbyshire E (ed) *Geomorphology and climate*. John Wiley & Sons, New York, pp 203–246
- Styczen ME, Morgan RPC (1995) Engineering properties of vegetation. In: Morgan RPC, Rickson RJ (eds) *Slope Stabilisation and erosion control: a bioengineering approach*. Spon, London, pp 5–58
- Swanston DN, Dyrness CT (1973) Stability of steep land. *Forest J* 71:264–269
- Tsukamoto Y, Ohta T (1988) Runoff processes on a steep forested slope. *J Hydrol* 102:165–178
- Terlien MTJ, van Asch TWJ, van Westen CJ (1995) Deterministic modelling in GIS–based landslide hazard assessment. In: Carrara A, Guzzetti F (eds) *Geographical information systems in assessing natural hazards*. Kluwer Academic Publishing, Dordrecht, pp 57–77
- Terlien MTJ (1998) The determination of statistical and deterministic hydrological landslide-triggering thresholds. *Environ Geol* 35:125–130
- Văn TT, Tuy PK, Giáp NX, Kế TD, Thái TN, Giang NT, Thọ HM, Tuấn LT, San DN, Hùng LQ, Chung HT, Hoan NT et al (2001) Assessment and prediction of geohazards in the 8 coastal provinces of Central Vietnam from Quang Binh to Phu Yen: present situation, causes, prediction and recommendation of remedial measures. *Investigation and Mitigation Resources, Hanoi*
- van Asch TWJ, Van Beek LPH, Bogaard TA (2009) The diversity in hydrological triggering systems of landslides. In: Picarelli L, Tommasi P, Urciuoli G, Versace P (ed) *Rainfall–induced landslides: mechanisms, monitoring techniques and nowcasting models for early warning systems*. *Proc 1st Italian Workshop on Landslides, Naples*, 8–10 June 2009, pp 151–157
- van Westen CJ (1994) GIS in landslide hazard zonation: a review, with examples from the Andes of Colombia. In: Price MF, Heywood DJ (eds) *Mountain environments and geographic information systems*. Taylor and Francis Publishers, London, pp 135–165
- van Westen CJ, Terlien MTJ (1996) An approach towards deterministic landslide hazard analysis in GIS: a case study from Manizales, Colombia. *Earth Surf Process Landform* 21:853–868
- van Westen CJ, Rengers N, Terlien MTJ, Soeters R (1997) Prediction of the occurrence of slope instability phenomena through GIS–based hazard zonation. *Geol Rundsch* 86:404–414
- van Westen CJ, Van Asch TWJ, Soeters R (2006) Landslide hazard and risk zonation—why is it still so difficult? *Bull Eng Geol Environ* 65:167–184
- van Westen CJ, Castellanos E, Kuriakose SL (2008) Spatial data for landslide susceptibility, hazard, and vulnerability assessment: an overview. *Eng Geol* 102:112–131
- Varnes DJ (1978) Slope movements, types and processes. In: Schuster RL, Krizek RJ (eds) *Landslide analysis and control*. National Academy Sciences, Washington, pp 11–33
- Varnes DJ, International Association of Engineering Geology Commission on Landslides and other Mass Movements (1984) *Landslide hazard zonation: a review of principles and practice*. UNESCO Press, Paris
- Vinh BL (2007) Regional slope instability zonation using different GIS techniques. Vrije Universiteit Brussel
- Wu W, Sidle RC (1995) A distributed slope stability model for steep forested basins. *Water Resour Res* 31:2097–2110
- Wu TH, McKinnel WP, Swanston DN (1979) Strength of tree roots and landslides on Prince of Wales Island, Alaska. *Can Geotec J* 16:19–33

L. N. Thanh · F. De Smedt (✉)

Department of Hydrology and Hydraulic Engineering,
Vrije Universiteit Brussel,
Brussels, Belgium
e-mail: fdesmedt@vub.ac.be

L. N. Thanh
e-mail: ntlongq1974@yahoo.com

L. N. Thanh
Remote Sensing and Geomatics Department,
Vietnam Institute of Geosciences and Mineral Resources,
Hanoi, Vietnam